

Antiproton stopping power in hydrogen below 120 keV and the Barkas effect

A. Adamo,^a M. Agnello,^b F. Balestra,^c G. Belli,^d G. Bendiscioli,^e A. Bertin,^f
 P. Boccaccio,^g G. C. Bonazzola,^c T. Bressani,^c M. Bruschi,^f M. P. Bussa,^c L. Busso,^c D. Calvo,^c
 M. Capponi,^f C. Cicalò,^a M. Corradini,^d S. Costa,^c I. D'Antone,^f S. De Castro,^f F. D'Isep,^c
 A. Donzella,^d I. V. Falomkin,^h L. Fava,^c A. Feliciello,^c L. Ferrero,^c V. Filippini,^e D. Galli,^f
 R. Garfagnini,^c U. Gastaldi,^g P. Gianotti,^c A. Grasso,^c C. Guaraldo,ⁱ F. Iazzi,^b A. Lanaro,ⁱ
 E. Lodi Rizzini,^d M. Lombardi,^g V. Lucherini,ⁱ A. Maggiora,^c S. Marcello,^c U. Marconi,^f G. Maron,^g
 A. Masoni,^a I. Massa,^f B. Minetti,^b M. Morando,^j P. Montagna,^e F. Nichitiu,^h D. Panzieri,^c
 G. Pauli,^k M. Piccinini,^f G. Piragino,^c M. Poli,^l G. B. Pontecorvo,^h G. Puddu,^a R. A. Ricci,^{g,i}
 E. Rossetto,^c A. Rotondi,^e A. M. Rozhdestvensky,^h P. Salvini,^c L. Santi,^m M. G. Sapozhnikov,^h N. Semprini Cesari,^f
 S. Serici,^a P. Temnikov,^h S. Tessaro,^k F. Tosello,^c V. I. Tretyak,^{e,h} G. L. Usai,^a L. Vannucci,^g
 G. Vedovato,^g L. Venturelli,^d M. Villa,^f A. Vitale,^f G. Zavattini,^f A. Zenoni,^c A. Zoccoli,^f and
 G. Zosi^c

(OBELIX Collaboration)

^aDipartimento di Scienze Fisiche, Università di Cagliari, Cagliari, Italy
 and Istituto Nazionale di Fisica Nucleare, Sezione di Cagliari, I-09100 Cagliari, Italy

^bPolitecnico di Torino, Torino, Italy

and Istituto Nazionale di Fisica Nucleare, Sezione di Torino, I-10150 Torino, Italy

^cIstituto di Fisica, Università di Torino, Torino, Italy

and Istituto Nazionale di Fisica Nucleare, Sezione di Torino, I-10125 Torino, Italy

^dDipartimento di Elettronica per l'Automazione, Università degli Studi di Brescia,
 and Istituto Nazionale di Fisica Nucleare, Sezione di Torino, I-25133 Brescia, Italy

^eDipartimento di Fisica Nucleare e Teorica, Università di Pavia,

and Istituto Nazionale di Fisica Nucleare, Sezione di Pavia, I-27100 Pavia, Italy

^fDipartimento di Fisica, Università di Bologna,

and Istituto Nazionale di Fisica Nucleare, Sezione di Bologna, I-40100 Bologna, Italy

^gLaboratori Nazionali di Legnaro dell'Istituto Nazionale di Fisica Nucleare, I-35020 Legnaro (Padova), Italy

^hJoint Institute for Nuclear Research, Dubna, SU-101000 Moscow, Russia

ⁱLaboratori di Frascati dell'Istituto Nazionale di Fisica Nucleare, I-00044 Frascati, Italy

^jDipartimento di Fisica, Università di Padova,

and Istituto Nazionale di Fisica Nucleare, Sezione di Padova, I-35100 Padova, Italy

^kIstituto di Fisica, Università di Trieste,

and Istituto Nazionale di Fisica Nucleare, Sezione di Trieste, I-34127 Trieste, Italy

^lDipartimento di Energetica, Università di Firenze, Firenze, Italy

and Istituto Nazionale di Fisica Nucleare, Sezione di Bologna, I-40100 Bologna, Italy

^mIstituto di Fisica, Università di Udine,

and Istituto Nazionale di Fisica Nucleare, Sezione di Trieste, I-33100 Udine, Italy

(Received 27 July 1992)

The simultaneous measurement of the spatial coordinates and times of \bar{p} s annihilating at rest in a H_2 target at very low density ρ ($\rho/\rho_0 < 10^{-2}$, ρ_0 being the STP density) gives the possibility of evaluating the behavior of the \bar{p} stopping power in H_2 at low energies (below 120 keV). It is different from that of protons (the Barkas effect). Moreover, it is shown that a rise at low-energy values ($\lesssim 1$ keV) is needed to agree with experimental data.

PACS number(s): 34.50.Bw

Following the original work of Bohr [1] the high-energy (projectile velocity $\gg e^2/\hbar$) behavior of the stopping power is very well described by the Bethe [2] formula for a point charge penetrating through matter at non-relativistic speed; it is proportional to the projectile charge squared (Z_1^2). Focusing on protons and antiprotons (\bar{p}) as projectiles at low velocity ($v \approx e^2/\hbar$) the Born

series is generally assumed to fail and other methods of calculating the consequences of collision are required. At very low velocity ($v < e^2/\hbar$) a proton loses energy not only in electronic collisions which lead to excitation and ionization; elastic scattering by the screened nuclei is also important. For protons, the electronic stopping power has a maximum around the typical electron velocity, i.e.,

≈ 55 keV for H_2 . Around and below the maximum, measurements are not well reproduced by theoretical estimates. The electronic contribution to the total energy loss in hydrogen is commonly assumed (e.g., in published tabulations [3]) to decrease linearly with the proton velocity for energies below 10 keV; see also Ref. [4].

For antiprotons, even the qualitative behavior of the stopping power is only poorly evaluated [5–9]. For \bar{p} 's at very low velocities, the energy loss due to excitation and ionization is expected to be considerably enhanced due to the so-called adiabatic ionization processes (see Refs. [5–7]). For close collisions the passage of a \bar{p} inside the orbital radius of a target electron will reduce the effective nuclear charge seen by the electron which will lead to a release of the electron. This fact was first pointed out by Fermi and Teller [10], who specifically considered the ground state of a system consisting of a negative muon and a molecule. The molecular mechanism peculiar to the case of hydrogen has been worked out by Wightman [5]. For antiprotons colliding with atomic hydrogen, Kimura and Inokuti [6] used a molecular-orbital expansion method to show that if the antiproton comes within a distance $R_x = 0.64a_0$ (a_0 is the Bohr radius, 0.053 nm) from the proton, then the target is ionized (the same R_x was found by Fermi and Teller).

Furthermore, a difference in the stopping power for positive and negative particles (the Barkas effect) [11] has been known for a long time, but lack of suitable antiparticle beams has prohibited quantitative studies [12–23] of the effect until recent years [24–26].

With the advent of LEAR (low-energy antiproton ring) at CERN, a high-quality beam of antiprotons at low energies became available, permitting accurate measurements of the stopping power for antiprotons down to 200 keV [24–26] and their ionization [27–29].

To study $\bar{p}p$ annihilations at rest, the OBELIX collaboration [30] has realized a very low-density hydrogen target, the ratio between the experimental density ρ and the STP density ρ_0 ranging from 10^{-2} to 10^{-3} , and a total of some 10^5 annihilation events has been collected. These data are of great interest for the evaluation of the \bar{p} stopping power particularly from the energy region just above the maximum down to some hundreds of eV.

The LEAR machine delivers to our experiment a monochromatic 105-MeV/c \bar{p} beam, which passes through some materials (a Be window closing the beam pipe, a thin scintillator detector S_0 , variable air, and Mylar sheets) before entering the ultrapure (less than 1 ppm of other gases) hydrogen target, 75 cm long and 30 cm in diameter. To maximize the fraction of \bar{p} s annihilating at rest in the target it is desirable that the largest number of \bar{p} s enter the target volume with a narrow momentum bite and the appropriate nominal momentum. In the best arrangement $\approx 45\%$ of \bar{p} s are stopped in the Mylar window at the entrance of the target and the remaining ones enter the target volume with a momentum spectrum ranging from 0 to ≈ 43 MeV/c. We measure this value with an empty target ($< 10^{-5}$ mbar) by time of flight. More details of the experimental technique are given in Ref. [30]. We have used three H_2 pressure values ($p_1 = 8.20 \pm 0.05$, $p_2 = 4.10 \pm 0.05$, $p_3 = 2.10 \pm 0.05$ mbar) to which corre-

spond three different $E^{\max}(p_j)$ for the kinetic energy of \bar{p} s stopping and annihilating in the H_2 gas just before the end of the target. More important, the energy spread (from the minimum zero energy at the entrance) produces a distribution of the stopping points of the \bar{p} s in the (z, t) plane.

Figure 1 shows the distribution of the experimental mean annihilation times (t_a) in the target as a function of the path length (along the z beam direction) for the three values of the pressure. Experimentally, t_a for each event is measured by the time at which the charged particles produced in the annihilation hit the scintillator barrel surrounding the target, relative to the starting time t_0 given by the \bar{p} crossing the beam scintillator counter. The time resolution is better than 1 ns. The annihilation times distributions are convolutions between the times of moderation (t) until the \bar{p} s capture and the cascade times (t_{cas}) of the protonium atoms. We plotted the distribution of t_a corresponding to a bin in z of 2 cm, the experimental spatial resolution being 1 cm. We found that all the distributions obtained in this way, well populated statistically, had a constant width and were fully consistent with Gaussian distributions (see Fig. 2). As discussed in Ref. [30], this circumstance allowed us to determine the $(\bar{p}p)$ atom cascade widths. Furthermore, it indicates that a continuous slowing down picture for the \bar{p} stopping power, $S(E)$, may well be adopted. The error on the experimental mean values of t_a for each bin in z is negligible.

The experimental information contained in Fig. 1 may well be related to S of \bar{p} . In fact the \bar{p} total path length R is evaluated by integration of S ,

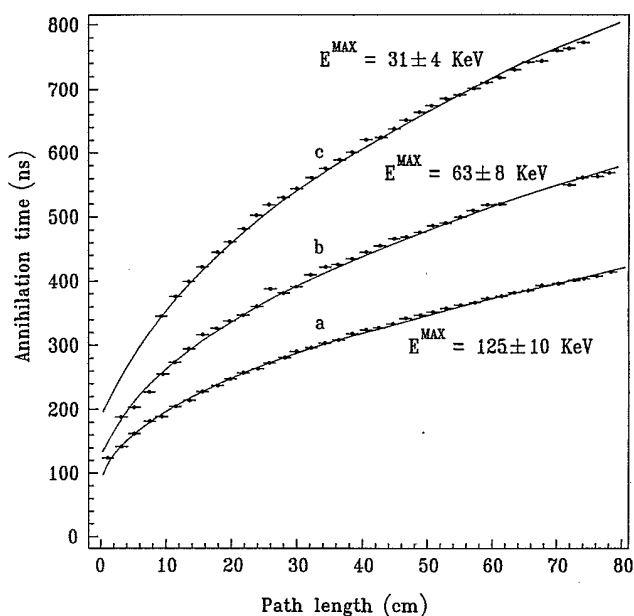


FIG. 1. Bidimensional distributions of the mean $\bar{p}p$ annihilation times (t_a) in the target as a function of the annihilation coordinate z for 8.2 mbar, curve a , 4.2 mbar, curve b , and 2.1 mbar, curve c H_2 pressure values compared with the results of our best-fitting function; see Fig. 3.

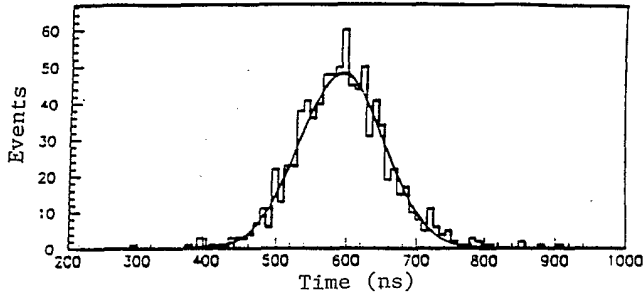


FIG. 2. A typical experimental annihilation time distribution for a 2-cm-wide bin for events in the target at a H_2 pressure of 2.1 mbar.

$$R = \int_{\bar{E}_{\text{cap}}}^{E_i} \frac{dE}{S(E)} \quad (1)$$

and, analogously, the mean moderation time t by

$$t = t_a - t_{\text{cas}} = \int_{\bar{E}_{\text{cap}}}^{E_i} \frac{dE}{vS(E)}, \quad (2)$$

E_i being the variable kinetic energy of each \bar{p} at the beginning of the target.

Two parameters enter in the annihilation distributions in the target, apart from S : (i) the mean kinetic energy of \bar{p} s captured by protons (\bar{E}_{cap}) and (ii) the mean cascade time of the $(\bar{p}-p)$ atom, $(t_a - t)$, which is different at the three pressures; see Ref. [30]. The experimental data are the $(R_i, t_i + t_{\text{cas}})$ mean values for the three situations; $0 \leq E_i \leq E^{\text{max}}(p_j)$ with $E^{\text{max}}(p_3) < E^{\text{max}}(p_2) < E^{\text{max}}(p_1)$. We outline that, contrary to what was done with different probes (e.g., μ^\pm), S is determined, with our technique, by the *simultaneous* solution of both space and time relationships (1) and (2). This is possible only with \bar{p} s, due to their specific feature of the annihilation and with a sophisticated and complete apparatus like OBELIX. In particular, the use of (2) allows us to avoid ambiguities or corrections inevitable in measurements in which only the spatial coordinate relationship (1) is used, and then S is derived from the projected range and not from the total range. Moreover, even if we suppose that around 10% of events (typically with the higher annihilations times in any 2-cm-wide bin) are characterized by a greater total path length and the proper positioning would be in the neighboring bin, our distributions in practice do not change.

By numerical integration and with $\bar{E}_{\text{cap}} \leq 10$ eV (see, e.g., Ref. [31]), we have obtained the best fit to the data (solid line in Fig. 1) by means of the well-known parametrization [3] $S^{-1} = S_{\text{low}}^{-1} + S_{\text{high}}^{-1}$, with $S_{\text{low}} = \alpha E^\beta$ and $S_{\text{high}} = (242.6/E) \ln(1 + 1.2 \times 10^4/E + 0.1159E)$, E being measured in keV. The fit was performed for the data between 0.7 and 120 keV and we obtained $\chi_r^2 = 0.57$ (99 degrees of freedom). Other parametrization functions furnished bad values of χ^2 . So, our methodology makes it possible to argue quantitatively that the present result is a good approximation to the real stopping power. Figure 3 shows a comparison of the best-fitting function (curve b)

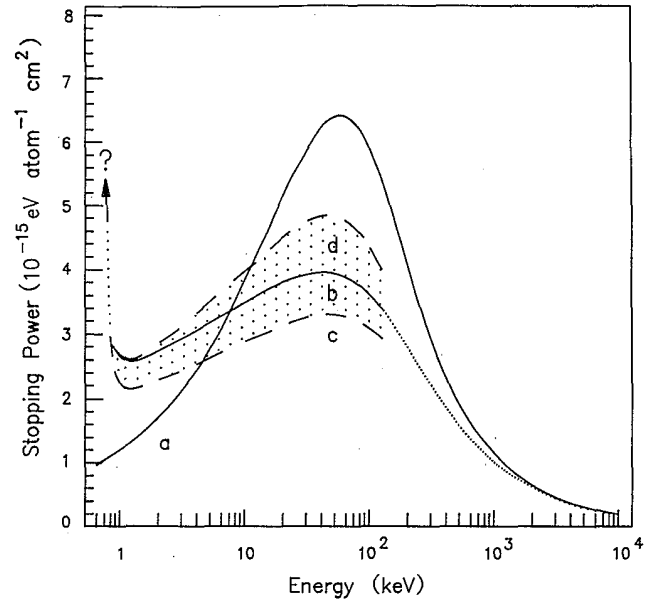


FIG. 3. Comparison between the proton stopping power in H_2 , curve a from Ref. [3], and the region (the dotted area) of acceptable behaviors for the antiproton one. Curve b is our best-fitting function and curves c and d are examples of limiting acceptable behaviors. A fast rise below 0.7 keV, necessary to explain the data but not used in the fit, is indicated by a dotted line.

with that for the proton (curve a).

The best-fitting value for S_{low} did not affect the behavior of S at high energies. Its relative importance is, e.g., 1% at 10 MeV.

Furthermore, an increase of S below 0.7 keV is necessary in order to explain the experimental data. This is clearly shown in Fig. 4. It appears that, even by assum-

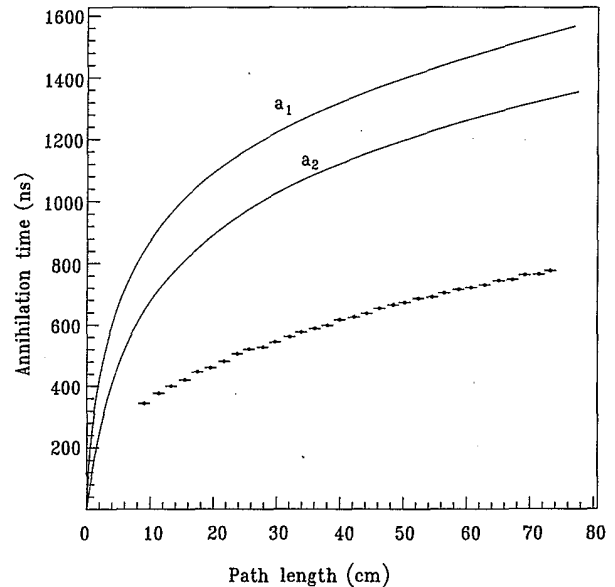


FIG. 4. Comparison between experimental data at 2.1 mbar hydrogen pressure and proton behavior after Andersen and Ziegler [3], with $\bar{E}_{\text{cap}} \leq 10$ eV, $t_{\text{cas}} = 200$ ns, curve a_1 , and $t_{\text{cas}} = 0$ ns, curve a_2 .

ing $t_{\text{cas}}=0$, no agreement with the data can be obtained by using an extrapolation down to zero proportional to v , as used for protons by Andersen and Ziegler [3]. This conclusion is independent from the circumstance that in (1) we use R projected, that we measure, instead of R . In order to explain the experimental data without a fast rise of S we would need a reduction (and not an increase) of R by a factor 10.

The following remarks may be drawn.

(i) Between 10 and 120 keV the mean \bar{p} stopping power in H_2 is systematically lower than that of proton. We recall that Sørensen [9] evaluated \bar{p} stopping power about half that of proton below the stopping maximum.

(ii) The maximum in the \bar{p} stopping power is $\approx(60\pm13)\%$ of that for proton.

(iii) The \bar{p} stopping power crosses that of the proton below 10 keV.

(iv) With such a \bar{p} stopping-power behavior, the cascade times at the three pressures p_1 , p_2 , and p_3 turn out

to be 100 ± 10 , 135 ± 15 , and 200 ± 25 ns, in good agreement with our previous conclusions [30].

In conclusion, the Barkas effect for hydrogen shows up clearly. We answer positively also as to the existence of a maximum in the antiproton stopping power, as for proton, a question that has been posed; see, e.g., Refs. [9,16]. Finally a fast rise of the stopping power below 0.7 keV is observed, in agreement with the qualitative previsions [6,7] originally proposed by Fermi and Teller [10], and evaluated for hydrogen by Wightman [5]. A rise of the stopping power near zero kinetic energy was highlighted in the μ^- stopping cross section evaluation by Cohen [32], and indicated also by the indirect measurement of the energy loss of μ^- in helium by Kottmann [33].

Many thanks are due to Professor E. Zavattini for useful discussions and suggestions, and to Professor G. Manuzio for valuable discussions during the preparation of this manuscript.

-
- [1] N. Bohr, *Philos. Mag.* **25**, 10 (1913).
 - [2] H. Bethe, *Ann. Phys. (Leipzig)* **5**, 325 (1930).
 - [3] *Hydrogen Stopping Powers and Ranges in All Elements*, edited by H. H. Andersen and J. F. Ziegler (Pergamon, New York, 1977).
 - [4] R. Golser and D. Semrad, *Nucl. Instrum. Methods B* **69**, 18 (1992).
 - [5] A. S. Wightman, *Phys. Rev.* **77**, 521 (1950).
 - [6] M. Kimura and M. Inokuti, *Phys. Rev. A* **38**, 3801 (1988).
 - [7] D. L. Morgan, Jr., *Hyperfine Interact.* **44**, 399 (1988).
 - [8] A. M. Ermolaev, *Hyperfine Interact.* **44**, 375 (1988).
 - [9] A. H. Sørensen, *Nucl. Instrum. Methods B* **48**, 10 (1990).
 - [10] E. Fermi and E. Teller, *Phys. Rev.* **72**, 399 (1947).
 - [11] W. H. Barkas, J. N. Dyer, and H. H. Heckman, *Phys. Rev. Lett.* **11**, 26 (1963).
 - [12] J. C. Ashley, R. H. Ritchie, and W. Brandt, *Phys. Rev. B* **5**, 2392 (1972).
 - [13] J. Lindhard, *Nucl. Instrum. Methods* **132**, 1 (1976).
 - [14] G. Basbas, *Nucl. Instrum. Methods B* **4**, 227 (1984).
 - [15] C. D. Hu and E. Zaremba, *Phys. Rev. B* **37**, 9268 (1988).
 - [16] H. H. Mikkelsen and P. Sigmund, *Phys. Rev. A* **40**, 101 (1989).
 - [17] S. P. Møller, *Nucl. Instrum. Methods B* **48**, 1 (1990).
 - [18] H. H. Mikkelsen, H. Esbensen, and P. Sigmund, *Nucl. Instrum. Methods B* **48**, 8 (1990).
 - [19] H. H. Mikkelsen and E. H. Mortensen, *Nucl. Instrum. Methods B* **48**, 39 (1990).
 - [20] D. Semrad, Ch. Eppacher, and R. Tober, *Nucl. Instrum. Methods B* **48**, 79 (1990).
 - [21] H. Bichsel, *Phys. Rev. A* **41**, 3642 (1990).
 - [22] I. Nagy, B. Apagyi, and K. Ladanyi, *Phys. Rev. A* **42**, 1806 (1990).
 - [23] I. Nagy *et al.*, *Phys. Rev. B* **44**, 12 172 (1991).
 - [24] R. Medenwaldt *et al.*, *Nucl. Instrum. Methods B* **58**, 1 (1991).
 - [25] R. Medenwaldt *et al.*, *Phys. Lett. A* **155**, 155 (1991).
 - [26] L. H. Andersen *et al.*, *Phys. Rev. Lett.* **62**, 1731 (1989).
 - [27] L. H. Andersen *et al.*, *Phys. Rev. A* **41**, 6536 (1990).
 - [28] H. Knudsen and J. F. Reading, *Phys. Rep.* **212**, 107 (1992).
 - [29] R. Bacher *et al.*, *Phys. Rev. A* **38**, 4395 (1988).
 - [30] A. Adamo *et al.*, *Phys. Lett. B* **285**, 15 (1992).
 - [31] J. S. Cohen, *Phys. Rev. A* **36**, 2024 (1987).
 - [32] J. S. Cohen, *Phys. Rev. A* **27**, 167 (1983).
 - [33] F. Kottmann (unpublished).